Cross-platform calibration of SMMR, SSM/I and AMSR-E passive microwave brightness temperature

Liyun Dai[*a, b] , Tao Che[a]
[a]Cold and Arid Regions Environmental and Engineering Research Institute, Chinese Academy of Sciences, Lanzhou 730000, China
[b]Graduate University of the Chinese Academy of Sciences, Beijing 100039, China

ABSTRACT

The long time series of passive microwave satellite data (SMMR, SSM/I and AMSR-E) have provided important information about the earth surface science and climate research in the past three decades. Due to the update of satellite-based radiometers and their platforms, some systematic parameters are different, and there are biases among brightness temperature in different periods, which lead to inaccuracy of some parameters' retrieval. In order to obtain consistent brightness temperature datasets, and provide convenience for the researchers using these data, it is necessary to calibrate the brightness temperature from different sensors. Considering the difference between the variance of brightness temperature from different sensors on cold and warm region at the cross time, this paper analyzed the brightness temperature on the cold and warm region respectively. On the cold region, because the diurnal temperature variation is very small, the influence on brightness temperature caused by difference of the satellites overpass time during the overlap period can be ignored. The brightness temperature data at 18GHz and 37GHz channels of Nimbus-7 and 19GHz, 37GHz channels of DMSP on the Antarctic or the Greenland glacier during the overlap period were analyzed. On the warm region, due to the reason that the daily variance of temperature contributes a lot to the difference of brightness temperature from different sensors during the overlap period, the diurnal cycle of surface temperature on the Sahara desert region was analyzed, and base on it, the influence of temperature to brightness temperature was eliminated. Finally, considering the two regions, the cross coefficients of calibration were estimated.

Key words: Brightness temperature, Passive microwave, Cross-platform calibration, diurnal cycle of temperature, SMMR, SSM/I

1. INTRODUCTION

The passive microwave remote sensing has its special advantages in comparison with visual and infrared remote sensing. First, its longer wavelength that can penetrate through cloud and independence on solar radiance enable it to work at any time and any weather. Second, some objects are more sensitive to microwave than to visible and infrared light. Third, it can penetrate through snow and ice, forest, and soil in some extent to provide profile information. And, its high temporal resolution makes it wide prospect in large and global scale study. Therefore, passive microwave remote sensing has been widely applied in earth surface sciences.

The time series of multi-frequency, dual-polarized, spaceborne passive microwave brightness temperature extends from October 1978 to present (SMMR: 1978-1987, SSM/I: 1987-present, AMSR-E: 2002-present). These data have been proven valuable for the retrieval of a diverse range of geophysical parameters, such as sea ice concentration[1], snow depth/water equivalent[2][3], soil moisture[4], land surface temperature[5], vegetation indice[6], lake ice duration[7], and so on. The long-term datasets are suitable for relatively time series analysis and change detection. SMMR, SSM/I and AMSR-E brightness temperatures are available from the National Snow and Ice Data Center (NSIDC) in a common gridded projection- the equal-area scalable earth grid (EASE-Grid), which facilitates the use of a cross-platform time series for investigating variability and trends in derived parameters[8][9].

However, their slightly different spatial, temporal, and radiometric characteristics have impacts on brightness temperature continuity and consistency (Table 1). All these can lead to inaccuracy or error in deriving various surface parameters. Evaluation of this cross-platform time series using the algorithm developed by the meteorological service of Canada (MSC) for the retrieval of snow water equivalent on western north America, shows that SWE estimates derived

* Corresponding Author: Liyun Dai; dlydai@163.com

Sixth International Symposium on Digital Earth: Data Processing and Applications,
edited by Huadong Guo, Changlin Wang, Proc. of SPIE Vol. 7841, 784103
 · doi: 10.1117/12.873150

during SMMR winter seasons are systematically and significantly lower than retrievals during SSM/I seasons if no brightness temperature adjustments are employed[10]. When analyzing Seasonal variations in brightness temperature for central Antarctica, Van der Veen and Jezek [11] found that a -5K offset exists between the SMMR and SSM/I observations over Antarctica. To retrieve snow depth in the western China, the different coefficients within the algorithms should be

Table1. Comparison of the parameter from different sensors

	SMMR	SSM/I(F08)	SSM/I(F11)	SSM/I(F13)	AMSR-E
Platform	NIMBUS-7	DMSP-F08	DMSP-F11	DMSP-F13	EOS-Aqua
Time series	1978.10.26-1987.08.20	1987.7.9-1991.12.30	1991.12.3-1995.9.30	1995.5.3-	2002.6.19-
Channels(GHz)&Foot print(km)	18.7:55×41 37:27×18	19.35: 69×43 37: 37×28	19.35: 69×43 37: 37×28	19.35: 69×43 37: 37×28	18.7: 27×16 36.5: 14×8
Polarization	V & H	V & H	V & H	V & H	V & H
Cross/Along track interval	14×14to 56×28km	25×25km	25×25km	25×25km	18.7: 25km 36.5: 15km
Viewing Angle(°)	50.2	53.1	53.1	53.1	55
Data acquisition	Every other day	Daily	Daily	Daily	Daily
Swath width(km)	780	1400	1400	1400	1445
Approximate orbital timing(UTC)	Ascending-1200 equatorial crossing	Ascending-0600 equatorial crossing	Ascending-1800 equatorial crossing	Ascending-1800equatorial crossing	ascending-1330equatorial crossing

used in using SMMR and SSM/I brightness temperature [12]. Therefore, it is necessary to calibrate the cross-platform data.

A few studies examining this overlap period have been conducted, for example, Jezek adjusted SMMR 18- and 37-GHz channels based on comparisons with SSM/I brightness temperatures over Antarctica[13]. Mote adjusted SMMR 37H-GHz brightness temperatures using a regression equation developed over Greenland[14], and Bjorgo examined ice-covered pixels in the southern ocean[15]. Derksen use cold and warm overpass brightness temperatures to examine relatively warm terrestrial surfaces respectively [16]. The typical approach when standardizing cross-platform data is to use linear regression to identify the relationship between brightness temperatures from both sensors, with SSM/I F8 data serving as the baseline to which SMMR and subsequent SSM/I (F11& F13) sensors have been compared[13][17][18]. So far, the calibration of SSM/I and AMSR-E was not investigated.

Due to the overpass-time difference between two sensors, all above studies selected the region of extremely low temperature-the Antarctic or Greenland glacier as sample regions, which can ignored the influence caused by the daily temperature variance. Their results are not appropriate for other terrestrial applications with diurnally, and hence overpass-time sensitive properties. This study was to consider both warm and cold regions, and make a calibration between brightness temperatures from different sensors.

2. METHOD OF COMPARISON

Data sets used in this study were Ease-Grid SMMR and SSM/I brightness temperature data from NSIDC. Only complementary pairs of channel were compared, namely the SMMR 18H, 18V, 37H, 37V, SSM/I 19H, 19V, 37H, 37V, and AMSR-E 18H, 18V, 36H, 36V channels. The approach to standardize cross-platform data is to use linear regression to identify the relationship between brightness temperatures from both sensors. Spatial homogeneity is important, because the orbits of satellites have slightly different. The weak diurnal cycle is essential, because the instruments will not necessarily cross the same area at the same time of day. So, in the cold end, the vast polar ice sheets of Greenland and Antarctica satisfy these criteria. The methods of choosing samples in the hot end will be described in the section 2.2.

2.1 Data collection at cold end

As existing studies, co-located brightness temperatures over terrestrial surfaces of the Antarctic and Greenland ice sheets during two sensors overlap period were used as samples at the cold point. The overlap period of EASE-Grid data

from SMMR and SSM/I (F08) is from 2nd to 20th August, 1987, which is the cold season in south hemisphere. During the early part of the SSM/I mission, a geolocation problem was discovered with a magnitude of 25km or about 1 pixel. In order to void the geolocation problem, the eastern Antarctic land far from coast (Figure 1) was selected, in which the gradients in brightness temperature are less than 2K per pixel [11]. The difference of overpass time is 6h, only the cold overpass data were selected. There are 5002 matching grid cells.

The overlap period of EASE-Grid data from SSM/I(F08) and SSM/I(F11) is from the 7th to 15th in December, 1991, which is the cold season in north hemisphere. The middle part of the Greenland ice sheet was selected as sample regions (Figure 1). And only the data on cold overpass time were selected. There are 8591 matching grid cells. The cross period of EASE-Grid data from SSM/I(F11) and SSM/I(F13) is from 3rd in March to 1st in July, 1995, which is the cold season in north hemisphere. The eastern Antarctic land far from coast was selected as sample regions (Figure 1). Only when the time difference equals to zero, the data was selected, and the total number is 10023. The cross period of EASE-Grid data from SSM/I(F13) and AMSR-E is very long, this study selected the eastern Antarctic in June, 2003 only, on which the north hemisphere is cold season, and daily variance of temperature is small in the Antarctica. There are 8192 matching grid cells.

2.2 Data collection at hot end

In the warm regions, the Sahara desert was selected as sample regions. In this region, there are good spatial homogeneity and stability, but the temperature daily variance is significant, so the sampling method in cold region is not suitable. Here, the air temperature data from the National Climatic Data Center (NCDC) were used to remove the difference caused by air temperature at different overpass time. First, nine weather stations (Figure 1 and Table 2) were selected, around which the ground surface is fine homogeneity. Second, a model for diurnal variation in air temperature (Formula (1) and (2)) was used to simulate the air temperature at the station pixel at the overpass time [19]. Then, the relationship between the air temperature and brightness was built at these stations respectively. Finally, we used the relationship between air temperature and brightness temperature of F08, F11, F13 to correct brightness temperature of SMMR, F08, F11 and AMSR-E respectively. At last, the number of matching pairs of SMMR and F08, F08 and F11, F11 and F13, F13 and AMSR-E are 4486, 8864, 9069, 7801, respectively. Flow chart of comparison between SMMR and F08 can be described by Figure 2, while the comparison flow of the other three groups are similar to it.

$$T(h) = (T_{\max} - T_{\min}) \sin(\frac{\pi m}{y + 2a}) + T_{\min} \quad (1)$$

$$T(h) = T_{\min} + (T_{sunset} - T_{\min}) \exp(-\frac{bn}{z}) \quad (2)$$

Where y is day length (h), z is night length (h), $T(h)$ is temperature at the h-th hour, $T_{\max}$ and $T_{\min}$ are the maximum and minimum temperatures, T_{sunset} is the temperature at sunset, m is the number of hours after the minimum temperature occurs until sunset, n is the number of hours after sunset until the time of the minimum temperature, a equals to 1.86, b is 2.2, and we assume the minimum temperature occurs at 0.17h before sunrise.

Table2**.** Selected station in the Sahara desert

WMO number	605250	605590	605660	605710	605810	605900	606300	606800	606110
Lon	5.73E	6.78E	3.8E	2.25W	6.15E	2.87E	2.5E	5.43E	9.63E
Lat	34.8N	33.5N	32.4N	31.5N	31.67N	30.57N	27.23N	22.8N	28.05N

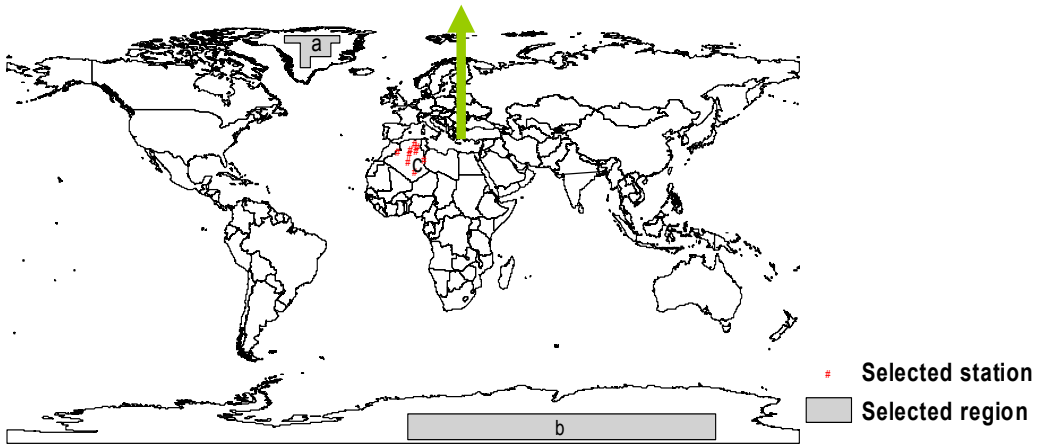

Fig. 1. Polygons are the selected sample areas at cold point, and points are selected station at hot point. Sample a in the Greenland glacier, and sample b in the Antarctic glacier, and c in the Sahara desert, table2 is the according station information**.**

3. RESULT

After selecting the data from cold and warm area, linear regression analysis was used to obtain the relationships between SMMR and F08, F08 and F11, F11 and F13, F13 and AMSR-E brightness temperatures in both cold and warm regions. The result was demonstrated from Figure 3 to 6 and the corresponding calibration coefficients were shown in Table 3.

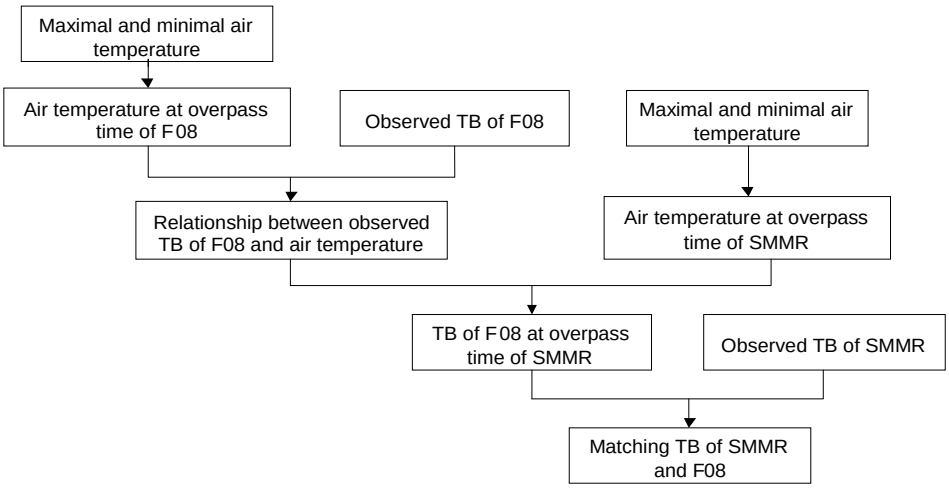

Fig. 2. Comparison progress of SMMR and F08 at hot end.

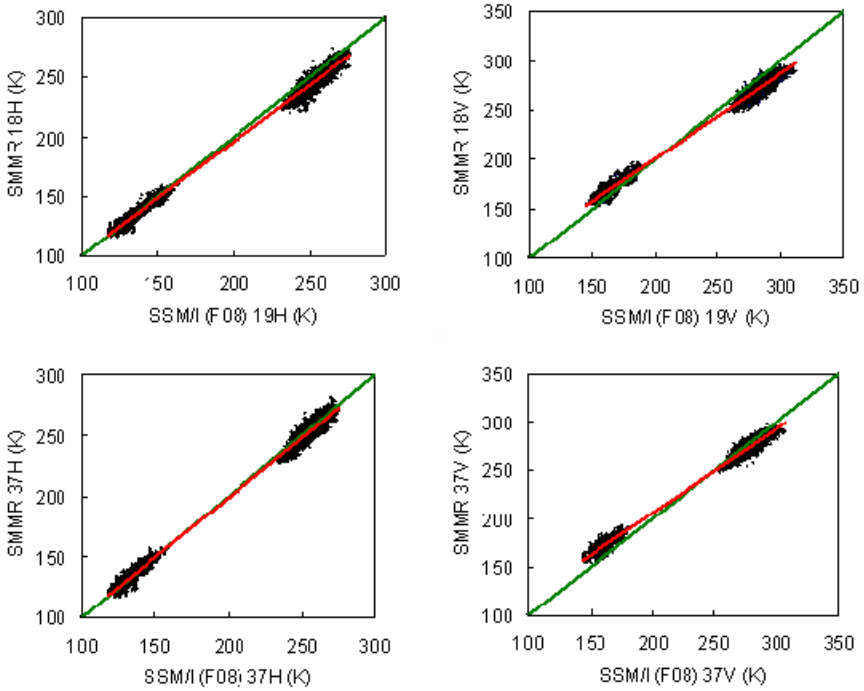

Fig. 3. Regression plots of brightness temperature of SMMR and SSM/I(F08).

It can be seen from the table 3 that the consistency among the three SSM/I sensors, and between SSM/I (F13) and AMSR-E are better than that between SMMR and SSM/I (F08). When the brightness temperature equal to 100K, differences between origin and adjusted data of 18HGHz, 18VGHz, 37HGHz, 37VGHz from SMMR are -2.2K, -18.15K, -1.77K, -22.641K respectively. When the brightness temperature equal to 300K, the differences between origin and corrected data are 11.14K, 16.66K, 4.3K, 10.02K.

When the brightness temperature equal to 100K, the differences from F08 are separately -0.34K, 0.89K, 0.16K, -0.06K, that from F11 are 0.16K, 0.28K, 0.23K, 0.05K, that from AMSR-E are 1K, 2.49K, 2.81K, 0.81K. When 300K, the differences from F08 are separately 0.58K, -0.23K, 1.6K, 0.86K, that from F11 are 0.52K, -0.38K, -0.13K, -0.47K, that from AMSR-E are 5.1K, -0.83K, -0.49K, -2.83K.

From above statistics, it can be seen that the differences among the three SSM/I and between SSM/I and AMSR-E brightness temperature are small. The overpass time of F11 and F13 are almost the same and the difference nearly equals to zero. The differences between F08 and F11, F13 and AMSR-E brightness temperature can be considered from the difference of overpass time of two cross platform and the error in modulation of the temperature at overpass time.

When compared to previous investigate results, it shows that the offset of SMMR and SSM/I (F08) is bigger when TB is 100K, and smaller when 300K. The offset of SSM/I(F08) and SSM/I(F11), SSM/I(F11) and SSM/I(F13) are smaller whenever TB is 100K or 300K.

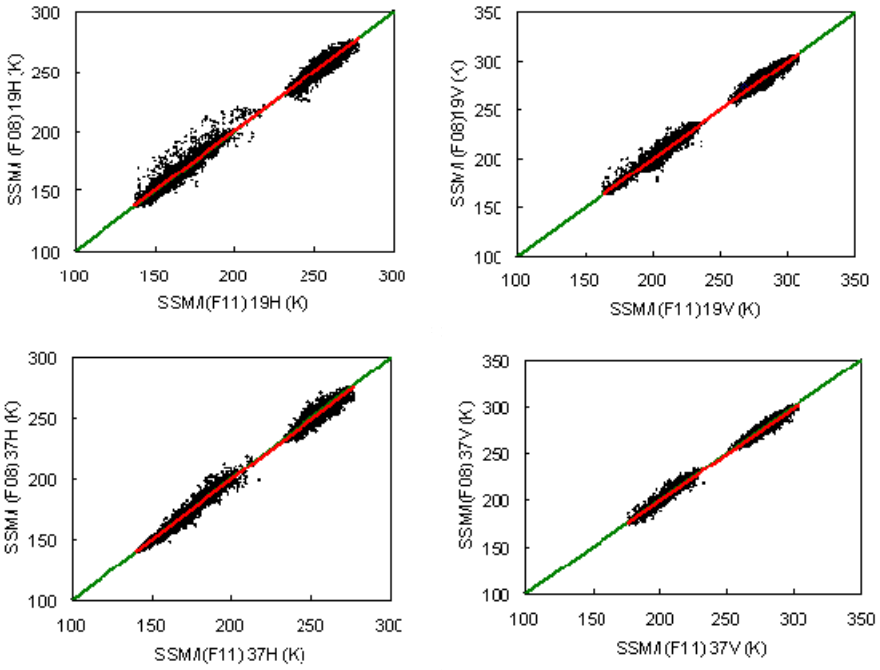

Fig. 4. Regression plots of brightness temperature of SSM/I(F08) and SSM/I(F11).

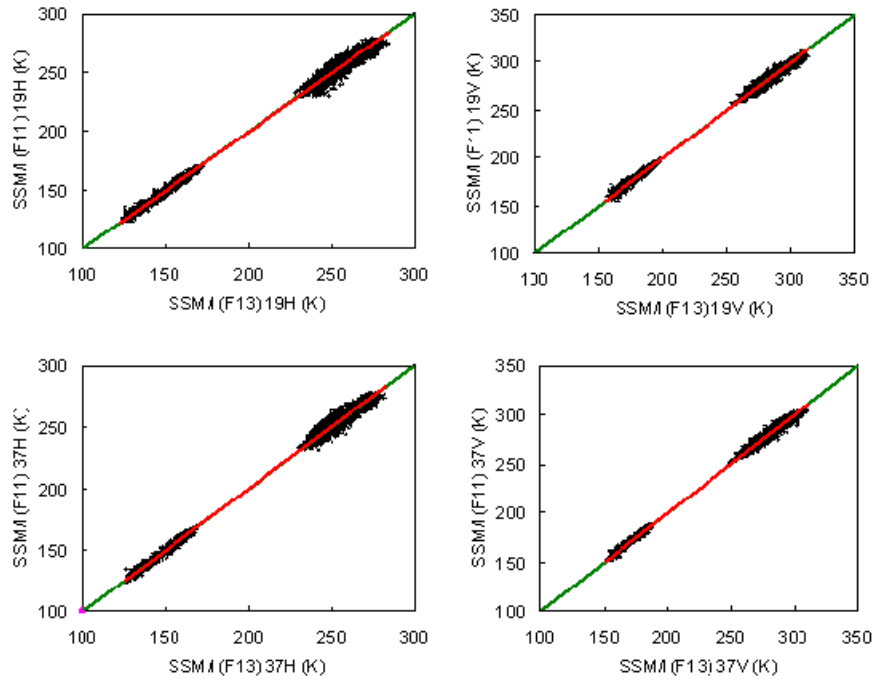

Fig. 5. Regression plots of brightness temperature of SSM/I(F11) and SSM/I(F13).

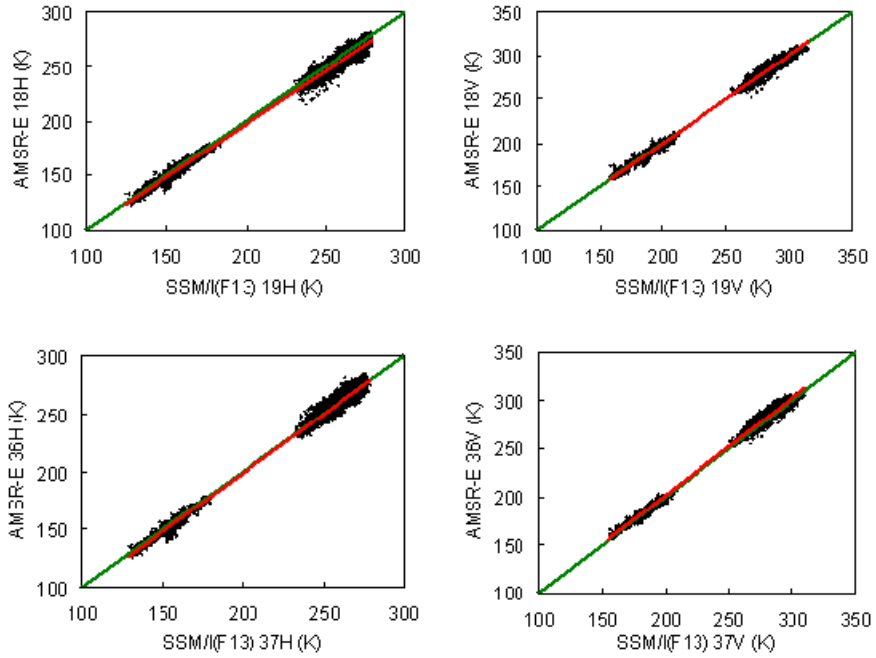

Fig. 6. Regression plots of brightness temperature of SSM/I(F13) and AMSR-E.

Table 3: Regression coefficients between two cross sensors. (a) coefficients between SMMR and SSM/I(F08), (b) coefficients between SSM/I(F08) and SSM/I(F11), (c) coefficients between SSM/I(F11) and SSM/I(F13), (d) coefficients between SSM/I(F13) and AMSR-E

(a)

Channel	Slope X=SMMR	Intercept (K) X=SMMR	R^2	Slope X=F08	Intercept (K) X=F08
18H/19H	1.0667	-8.8702	0.9967	0.9344	8.9173
18V/19V	1.174	-35.545	0.9955	0.848	31.134
37H/37H	1.0304	-4.8074	0.9968	0.9674	5.2716
37V/37V	1.1633	-38.971	0.9954	0.8557	34.361

(b)

Channel	Slope X=F08	Intercept (K) X=F08	R^2	Slope X=F11	Intercept (K) X=F11
19H	1.0046	-0.7998	0.9943	0.9898	1.9825
19V	0.9944	1.4489	0.9944	1.000	-0.0537
37H	1.0072	-0.5574	0.9959	0.9887	1.432
37V	1.0046	-0.5156	0.9964	0.9918	1.3799

(c)

Channel	Slope X=F11	Intercept (K) X=F11	R^2	Slope X=F13	Intercept (K) X=F13
19H	1.0018	-0.0222	0.9979	0.9961	0.4465
19V	0.9967	0.6073	0.9983	1.0016	-0.2237
37H	0.9982	0.4057	0.9984	1.0002	-0.0965
37V	0.9979	0.1588	0.9988	1.0009	-0.1041

(d)

Channel	Slope X=AMSR-E	Intercept (K) X=AMSR-E	R^2	Slope X=F13	Intercept (K) X=F13
18H/19H	1.0205	-1.0539	0.9962	0.9762	1.7888

18V/19V	0.9834	4.1518	0.9972	1.014	-3.5454
36H/37H	0.9835	4.4553	0.9967	1.0135	-3.8587
36V/37V	0.9818	2.6336	0.9973	1.0158	-2.0578

4. VALIDATION

In order to check the result, one pixel in the southern great plain in the USA was selected, of which the surface characteristics are mostly pasture and agricultural crops, with little topography variability, and comparison was made between the brightness temperature from SMMR and F08. The SMMR ascending overpass time at this pixel is at about 13:00, and the F08 descending overpass time is at about 19:00. The corresponding weather station named USC00346926 (LAT:34.73^{o}N, LON: 97.28^{o}W) come from NCDC, who includes the maximal and minimal surface air temperature. The temperature at the overpass time was evaluated based on formula (1) and (2). Obviously, the air temperature at 13:00 is higher than that at 19:00. (Figure7)

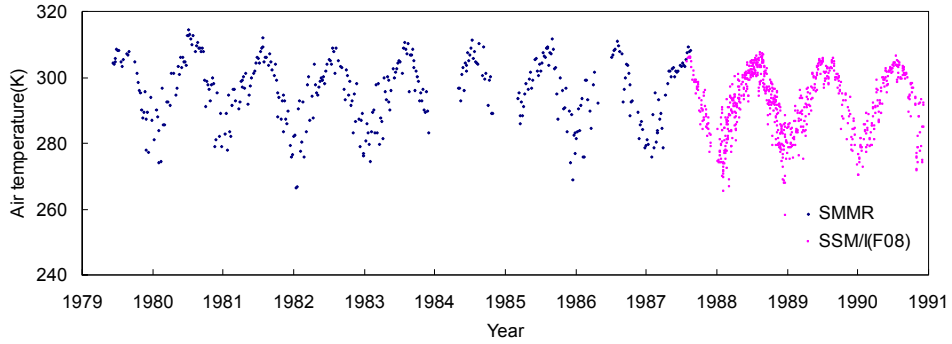

Fig. 7. The surface temperature at station USC00346926 (LAT: 34.73^{o}N, LON: 97.28^{o}W) in the south great plain in the USA at the overpass time. The overpass time of SMMR is about 13:00, SSM/I is about 19:00(SMMR: 1979-1986, F08: 1988-1991)

The brightness temperature data of SMMR and F08 at this pixel were extracted, and it was found that brightness temperature from SMMR of ascending orbit was lower than that from F08 of descending orbit, which is contrary to their surface air temperature. It could be described by figure 8. In this figure, the blue triangle present origin data, from which it can be seen the brightness temperature from 1979 to 1987(SMMR) is lower than from 1988 to 1990(F08) on every channel. The average brightness temperature of 18H, 18V, 37H, 37V from SMMR are 263.416K, 273.638K, 267.358K, 274.942K respectively, while the corresponding average brightness temperature from SSM/I(F08) are 271.245K, 278.627K, 270.207K, 275.344K. When the brightness temperature of SMMR was corrected based on the calibration coefficients in table3, it increased, the average brightness temperature are separately 272.379K, 285.711K, 270.279K, 280.869K, which are higher than that of F08, that is consistent with surface air temperature described in the figure7. The corrected brightness temperature data were presented by red diamond in figure8. So, the brightness temperature between SMMR and F08 should be cross calibrated when they were used to analyze in long time series.

5. CONCLUSION

The availability of a 30-year-plus satellite-based passive microwave brightness temperature time series in a common grid format is very attractive to the scientific community for investigating variability and change in derived geophysical parameters. The objective of this investigation is to identify any systematic bias between SMMR, SSM/I and AMSR-E, and unify them.

Regression analysis was performed on complementary channels of cross-platform brightness temperatures. From the calibration coefficients and statistics, it can be seen that there is highly consistence among SSM/I(S) and AMSR-E, and their difference can be ignored. The brightness temperature between SMMR and F08 should be cross calibrated when they were used to analyze in time series.

The long time series of passive microwave brightness temperature have great potential for addressing research problems that require a spatial dataset of significant length, and facilitates the use of long time series for investigating variability and trends in derived parameters. Further investigation is necessary to evaluate the impact of the brightness temperature

adjustments on derived variables such as snow depth or snow extent.

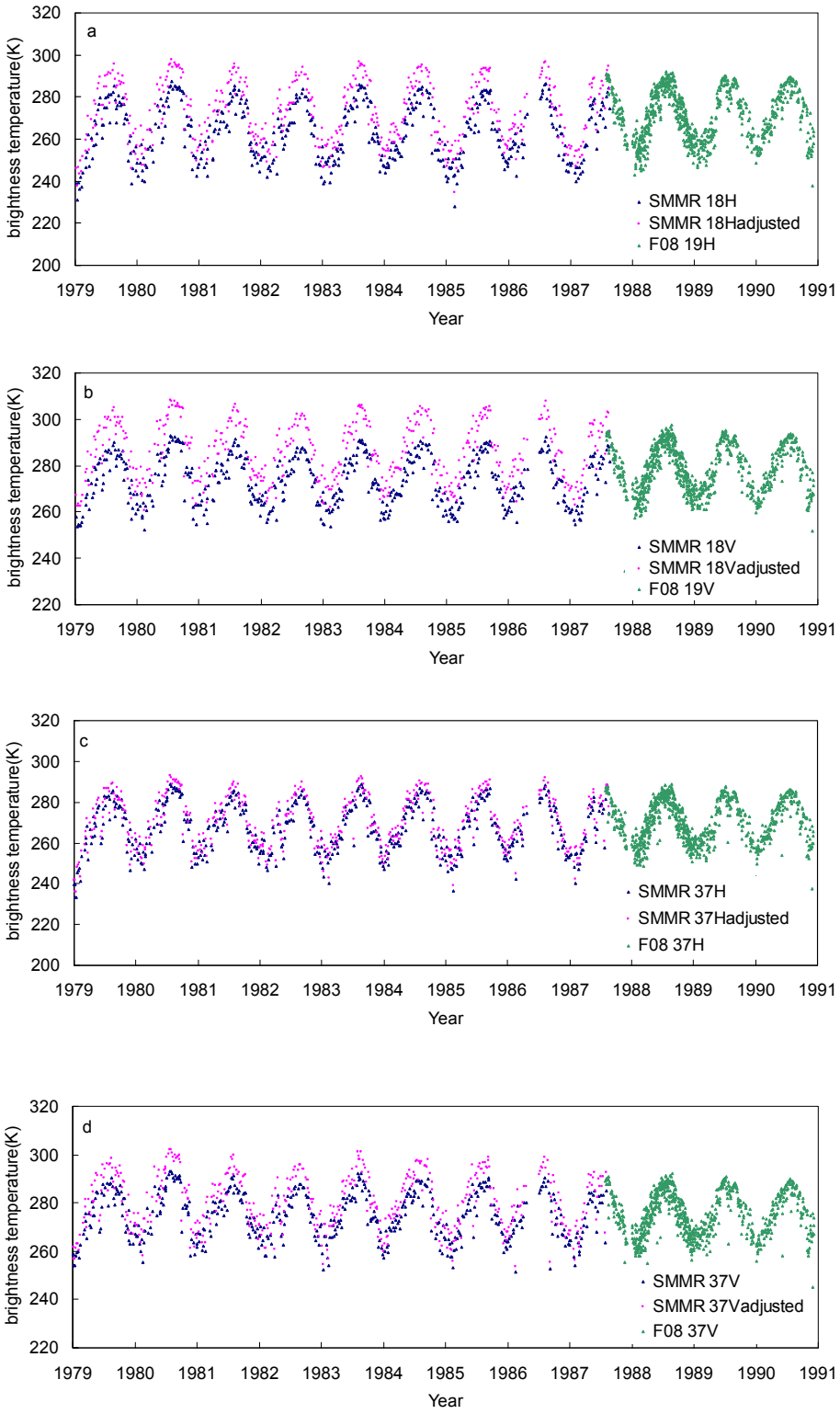

Fig. 8. Comparison between original and corrected brightness temperature. SMMR: 1979-1987, SSM/I: 1988-1990. (a) the Comparison of 18H/19H, (b) the comparison of 18V/19V, (c) the comparison of 37H, (d) the comparison of the 37V.

ACKNOWLEDGEMENTS

NSIDC provide the brightness temperature. NCDC provide the air temperature data. This work is supported by the China State Key basic Research Project (2007CB411506), the National Natural Science Foundation of China (40601065&40701030), and the open fund of State Key Laboratory of Cryosphere Sciences (SKLCS 08-01).

REFERENCES

[1] Comiso, J.C., Cavalieri, D.J., Parkinson, C.L. and Gloersen, P., "Passive microwave algorithms for sea ice concentration: A comparison of two thechniques," Remote sense of environment, vol.60, 357-384 (1997).

[2] Che, T., Li, X. and Gao, F., "Estimation of Snow Water Equivalent in the Tibetan Plateau Using Passive Microwave Remote Sensing Data (SSM/I)," Journal of Glaciology and Geocryology. Papers 26(3), 363–368 (2004).

[3] Che, T., Li, X., Gao, F. and Armstrong, R. L., "Study of snow water resources by passive microwave satellite data in China," Igarss 2004: IEEE International Geoscience and Remote Sensing Symposium Proceedings, Vols 1-7, 3674-3676(2004)

[4] Jackson, T.J., "soil moisture estimation using Special Sensor Microwave/Imager satellite data over a grassland region," Water Resources Res. Papers 33(6):1475-1484, (1997).

[5] Weng, F. and Grody, N.C., "Physical retrieval of land surface temperature using the Special Sensor Microwave Imager," J. Geophys. Res. Vol. 103, 8839-8848 (1998).

[6] Shi, J.C, Jackson, T., Tao, J., Du, J., Bindlish, R., Lu, L. and Chen, K.S., "Microwave vegetation indices for short vegetation cover from satellite passive microwave sensor AMSR-E," Remote Sensing of Environment. Papers 112(12), 4285-4300 (2008).

[7] Che, T., Li, X. and Jin, R. "Monitoring the frozen duration of Qinghai Lake using satellite passive microwave remote sensing low frequency data," Chinese Science Bulletin 54, 2294-2299(2009)

[8] Torinesi, O., Fily, M. and Genthon, C. "Interannual variability and trend of the Antarctic summer melting period from 20 years of spaceborne microwave data," Journal of Climate. Papers 16(7), 1047-1060 (2003).

[9] Picard, G. and Fily, M., "Surface melting observations in Antarctica by microwave radiometers: Correcting 26-year time series from changes in acquisition hours," Remote sensing of environment. Vol.104, 325-336 (2006).

[10] Derksen, C., LeDrew, E., Walker, A. and Goodison, B., "The influence of sensor overpass time on passive microwave retrieval of snow cover parameters," Remote Sens. Environ. Papers 71(3), 297–308 (2000).

[11] Van der Veen, C. J. and Jezek, K. C., "Seasonal variations in brightness temperature for central Antarctica," Annals of Glaciology. Vol.17, 300-306(1993).

[12] Che, T., Li, X., Jin, R., Armstrong, R.L. and ZHANG, T.J. , "Snow depth derived from passive microwave remote-sensing data in China," Annals of Glaciology. Vol.49, 145–154 (2008)

[13] Jezek, K., Merry, C. and Cavalieri, D., "Comparison of SMMRand SSM/I passive microwave data collected over Antarctica," Ann. Glaciol. Vol.17, 131-136 (1993).

[14] Mote, T. and Anderson, M., "Variations in snowpack melt on the Greenland ice sheet based on passive-microwave measurements," J. Glaciol. Papers 41(137), 51-60 (1995).

[15] Bjorgo, E., Johannessen, O. and Miles, M., "Analysis of merged SMMR-SSMI time series of Arctic and Antarctic sea ice parameters 1978-1995.Geophys," Res. Lett. Papers 24(4), 413-416 (1997).

[16] Derksen, C. and Walker, A.E., "Identification of Systematic Bias in the Cross-Platform (SMMR and SSM/I) EASE-Grid Brightness Temperature Time Series," IEEE Transactions on Geoscience and Remote sensing. Papers 41(4), 910-915 (2003).

[17] Abdalati, W., Steffen, K., Otto, C. and Jezek, K., "Comparison of brightness temperatures from SSMI instruments on the DMSP F8 and F11 satellites for Antarctica and the Greenland ice sheet," Int. J. Remote Sens. Papers 16(7), 1223-1229 (1995).

[18] Stroeve, J., Maslanik, J., and Li, X., "An intercomparison of DMSP F11 and F13-derived sea ice products," Remote Sens. Environ. Papers 64(2), 132-152 (1998).

[19] Parton, W.J. and Logan, J.A., "A model for diurnal variation in soil and air temperature," Agricultural Meteoroloy. Vol.23, 205-216 (1981).